Ecological Applications, 20(6), 2010, pp. 1569–1582

Looking deeper into the soil: biophysical controls and seasonal lags of soil CO_2 production and efflux

Rodrigo Vargas,[1,10] Dennis D. Baldocchi,[1] Michael F. Allen,[2] Michael Bahn,[3] T. Andrew Black,[4] Scott L. Collins,[5] Jorge Curiel Yuste,[6] Takashi Hirano,[7] Rachhpal S. Jassal,[4] Jukka Pumpanen,[8] and Jianwu Tang[9]

[1]*Department of Environmental Science, Policy, and Management, 137 Mulford Hall, University of California, Berkeley, California 94720 USA*
[2]*Center for Conservation Biology, University of California, Riverside, California 92521 USA*
[3]*Institute of Ecology, University of Innsbruck, Sternwartestrasse 15, 6020 Innsbruck, Austria*
[4]*Faculty of Land and Food Systems, University of British Columbia, Vancouver, British Columbia V6T 1Z4 Canada*
[5]*Department of Biology, MSC03-2020, University of New Mexico, Albuquerque, New Mexico 87131 USA*
[6]*Universidad Autónoma de Barcelona, Centre de Recerca Ecològica d'Aplicació Forestal (CREAF), Barcelona 08193 Spain*
[7]*Research Faculty of Agriculture, Hokkaido University, Sapporo 064-8589 Japan*
[8]*Department of Forest Ecology, University of Helsinki, Helsinki 00014 Finland*
[9]*The Ecosystems Center, Marine Biological Laboratory, Woods Hole, Massachusetts 02543 USA*

Abstract. We seek to understand how biophysical factors such as soil temperature (T_s), soil moisture (θ), and gross primary production (GPP) influence CO_2 fluxes across terrestrial ecosystems. Recent advancements in automated measurements and remote-sensing approaches have provided time series in which lags and relationships among variables can be explored. The purpose of this study is to present new applications of continuous measurements of soil CO_2 efflux (F_0) and soil CO_2 concentrations measurements. Here we explore how variation in T_s, θ, and GPP (derived from NASA's moderate-resolution imaging spectroradiometer [MODIS]) influence F_0 and soil CO_2 production (P_s). We focused on seasonal variation and used continuous measurements at a daily timescale across four vegetation types at 13 study sites to quantify: (1) differences in seasonal lags between soil CO_2 fluxes and T_s, θ, and GPP and (2) interactions and relationships between CO_2 fluxes with T_s, θ, and GPP. Mean annual T_s did not explain annual F_0 and P_s among vegetation types, but GPP explained 73% and 30% of the variation, respectively. We found evidence that lags between soil CO_2 fluxes and T_s or GPP provide insights into the role of plant phenology and information relevant about possible timing of controls of autotrophic and heterotrophic processes. The influences of biophysical factors that regulate daily F_0 and P_s are different among vegetation types, but GPP is a dominant variable for explaining soil CO_2 fluxes. The emergence of long-term automated soil CO_2 flux measurement networks provides a unique opportunity for extended investigations into F_0 and P_s processes in the near future.

Key words: lags; moderate-resolution imaging spectroradiometer (MODIS); photosynthesis; soil CO_2 efflux; soil CO_2 production; soil CO_2 sensors; soil respiration.

Introduction

Understanding the factors that influence patterns of terrestrial CO_2 fluxes across the globe is essential to predict and manage the effects of the human carbon footprint (Magnani et al. 2007). Soil CO_2 efflux (or soil respiration; F_0) constitutes a significant (10–90%) component of CO_2 fluxes from terrestrial ecosystems (Hanson et al. 2000), but the mechanistic understanding of F_0 remains unclear because of the complexity of processes involved. Here we present a synthesis study of the application of continuous automated measurements of soil CO_2 fluxes to identify lags and relationships among biophysical variables. Long-term continuous measurements provide an opportunity to understand how biophysical factors interact to regulate terrestrial CO_2 fluxes and provide an opportunity to explore the timing of biophysical controls on F_0. The application of continuous measurements of multiple biophysical variables will increase with the growth of environmental networks across multiple vegetation types (e.g., FLUXNET, National Ecological Observatory Network [NEON], Integrated Carbon Observation System [ICOS]).

Soil CO_2 efflux provides information about the interaction between soil processes and the atmosphere as an integrated result of biological CO_2 production at the soil surface and changes in soil CO_2 diffusivity in the soil profile. It is the result of the combined contribution of CO_2 production (P_s) in the soil by autotrophic (roots and mycorrhizae) and heterotrophic (decomposers)

Manuscript received 21 April 2009; revised 12 August 2009; accepted 4 November 2009. Corresponding Editor: D. S. Schimel.
[10] E-mail: rvargas@berkeley.edu

components (Hanson et al. 2000, Ryan and Law 2005) and diffusion of CO_2 through the porous medium. The diffusion of CO_2 in the soil is a function of exogenous factors that affect porosity and tortuosity, such as soil moisture, soil texture, and bulk density (Šimůnek and Suarez 1993, Moldrup et al. 1999, Pumpanen et al. 2003). Consequently, P_s provides information on biological activity because it represents the combined contribution of the autotrophic and heterotrophic components in the soil (Hanson et al. 2000, Ryan and Law 2005). Variation in P_s is mainly dependent on changes in root density, microbial community composition, quality and quantity of soil carbon pools, and photosynthetic activity (Kuzyakov 2006).

The influences of soil temperature (T_s) and soil water content (θ) have consistently been used to explain variation in F_0 at different temporal scales among vegetation types (e.g., Davidson et al. 2000, Curiel Yuste et al. 2003, Reichstein et al. 2003, Ma et al. 2005), and previous reviews have examined the influence of T_s and θ on F_0 (Raich et al. 2002, Hibbard et al. 2005, Ryan and Law 2005, Davidson and Janssens 2006). However, in most cases, previous studies have been based on manual CO_2 soil chamber measurements that miss multiple days of the year, night measurements, and precipitation events.

Recent technological advances with automated soil respiration chambers have greatly improved the time resolution of F_0 measurements (Goulden and Crill 1997, Drewitt et al. 2002, Irvine and Law 2002, Savage and Davidson 2003, Carbone et al. 2008). Alternatively, continuous belowground CO_2 concentration measurements using solid-state CO_2 sensors provide another method (flux-gradient method) for automated measurement of F_0 and P_s (Hirano et al. 2003, Jassal et al. 2004, Tang et al. 2005*b*, Pumpanen et al. 2008, Vargas and Allen 2008*a*). The flux gradient method has the advantage that F_0, soil CO_2 flux at depth i (F_i), and P_s can be calculated and compared with other methods (e.g., F_0 measured using the soil chamber method). Because of the challenge of measuring soil processes, only a few studies have investigated F_i and P_s (Davidson and Trumbore 1995, Hashimoto and Suzuki 2002, Takahashi et al. 2004, Fierer et al. 2005, Jassal et al. 2005, Pumpanen et al. 2008, Vargas and Allen 2008*c*), particularly with regard to variation in T_s (Risk et al. 2002, Hashimoto and Komatsu 2006).

Here we used measurements obtained by autochambers and solid-state CO_2 sensors in the soil profile to calculate F_0 and P_s in four vegetation types at 13 study sites. We concentrated on seasonal variation using mean daily values derived from continuous measurements that captured the seasonal influence of phenology (DeForest et al. 2006), temperature and water (Irvine and Law 2002), and photosynthesis (Högberg et al. 2001, Tang et al. 2005*a*, Bahn et al. 2009) on soil CO_2 fluxes. We investigate the influence of photosynthesis on F_0 and P_s among vegetation types using values of gross primary production (GPP) derived from NASA's moderate-resolution imaging spectroradiometer (MODIS; Running et al. 2004). We used GPP derived from MODIS because not all the sites included in this study have instrumentation of eddy covariance towers to measure GPP. (For a description of the eddy covariance network FLUXNET, see Baldocchi [2008].)

This study is novel in that it uses a unique data set on long-term continuous measurements of F_0 and P_s across multiple vegetation types to better understand how biophysical factors regulate soil CO_2 fluxes. An advantage of measuring soil CO_2 fluxes continuously with automated systems is the possibility to quantify lags between environmental variables and CO_2 fluxes (Baldocchi et al. 2006, Gaumont-Guay et al. 2006, Liu et al. 2006, Vargas and Allen 2008*a*). Using this information we ask two interrelated questions: (1) Are there seasonal lags between F_0 and T_s, GPP, or θ, and if so, do these lags differ among sites and vegetation types? (2) What are the relationships and interactions among F_0, T_s, θ, and GPP within different vegetation types?

Here we test three related hypotheses. H_1: Mean annual GPP (derived from MODIS) would be a better predictor of mean annual F_0 and P_s than mean annual T_s (measured in situ) across vegetation types. There is increasing evidence of the importance of GPP at multiple vegetation types (Janssens et al. 2001, Reichstein et al. 2003, Bahn et al. 2008), and it is relevant to explore the relationships between remote-sensing estimations and in situ measurements. H_2: Lags between F_0 and T_s or GPP can provide insights about possible timing of processes associated with autotrophic and heterotrophic components of F_0 (e.g., Braswell et al. 1997, McDowell et al. 2004, Baldocchi et al. 2006). We postulate that if F_0 increases with T_s and GPP (i.e., in phase with zero lags) there may be a synchronized temporal contribution of autotrophic and heterotrophic activity at the seasonal scale. In contrast, if F_0 increases before T_s (i.e., out of phase with negative lags) but after GPP (i.e., out of phase with positive lags) there may be different temporal controls for autotrophic and heterotrophic activity at the seasonal scale. The mechanisms that regulate lags at the seasonal scale could be driven by the different contributions of autotrophic and heterotrophic respiration, which are influenced by plant phenology (DeForest et al. 2006), photosynthesis (McDowell et al. 2004, Baldocchi et al. 2006, Bahn et al. 2009), and rhizosphere dynamics (Bahn et al. 2006, Gaumont-Guay et al. 2008, Vargas and Allen 2008*c*). H_3: The influence of biophysical factors on regulating daily F_0 and P_s is different among vegetation types, but general patterns may emerge, providing insights into the mechanisms that control soil CO_2 fluxes.

Materials and Methods

Study sites

We included data from 13 sites in which in situ solid-state soil CO_2 sensors are being used and all but two data

sets have been previously published in individual studies (Table 1). Sites were located in six countries between latitudes 61°50′ N and 21°12′ N and an altitudinal range from 70 to 1850 m above sea level. Mean annual temperatures ranged from 3° to 24°C, and annual precipitation ranged from 250 to 1650 mm (Table 2). All sites measured soil CO_2 concentrations at three or more depths except one grassland site that used automated soil respiration chambers in combination with two soil CO_2 sensors (Table 3). We grouped the study sites by vegetation types including three deciduous forests (DF), four evergreen coniferous forests (ECF), four grasslands (GRA), and two mixed forests (MF; see Table 1). This categorical classification follows physiological and morphological traits, and in most cases grouped sites share similar mycorrhizal associations. Furthermore, the characteristics of evergreen, deciduous, deciduous mixed forest, and grassland are observable from remote-sensing platforms (e.g., MODIS) and are key ecological properties for the determination of photosynthesis and respiration. The results from this study must be corroborated in the future using a larger network of sites with continuous measurements of soil CO_2 fluxes across multiple climatic zones and vegetation types.

Field measurements of soil CO_2 concentrations

Soil CO_2 measurements were collected between 2000 and 2007, depending on the study site; dates used in this study are reported in Table 3. At each site, soil CO_2 was continuously measured (mean hourly values) with Vaisala CARBOCAP CO_2 sensors (models GMM 222, GMM 221, GMT 222, GMD 20, or GMP 343; Vaisala, Helsinki, Finland) at multiple depths ranging between 0 and 50 cm (see Table 3). These small silicon-based CO_2 sensors operate on the nondispersive infrared (NDIR) single-beam dual-wavelength principle. The sensors were calibrated periodically against reference gases, and calibration details are reported in the main references for each site (Table 1). In most cases, the sensors were protected either with microporous Teflon tubing or Gore-Tex fiber to avoid possible wetting during rainfall events while allowing free gas exchange. Soil temperatures (in degrees Celsius) were measured at the same depths at which the CO_2 sensors were installed. Soil water content (in cubic meters per cubic meter) was measured either at the same depth as the CO_2 sensors or within the range of their deployment (e.g., 2–16 cm depth). Values of concentration of CO_2 were automatically corrected for temperature in the case of the GMP 343 sensors and corrected for temperature (other than the GMP 343) and pressure using the ideal gas law according to the manufacturer (Vaisala, Helsinki, Finland). To reduce noise of measured CO_2 concentrations being amplified in the calculation of F_0 and P_s, we applied a Savitzky-Golay smoothing filter, which preserves peak heights and widths of the original signal. A similar approach was used by Vargas et al. (*in press*) for continuous measurements of CO_2 concentrations.

Soil CO_2 efflux and soil CO_2 production

Soil CO_2 efflux values were obtained using automated soil respiration chambers (sites DF49, HDF88, Hyy, and Stu) or the flux gradient method (for the remaining sites; Table 3). Soil CO_2 production values were calculated from soil CO_2 concentrations using the flux gradient method in all sites. The flux gradient method has been verified using the soil chamber method at each site and is discussed in the main sources for each site (Table 1). Automated soil respiration chambers have been widely used for several years (Drewitt et al. 2002, Savage and Davidson 2003, Pumpanen et al. 2004), and descriptions of these systems at each study site are also available in the main sources provided in Table 1.

When F_0 or P_s values were calculated with soil CO_2 concentrations we used flux gradient theory (DeJong and Schapper 1972). This method is based on Fick's law of diffusion:

$$F = -D_s \frac{\partial C}{\partial z} \tag{1}$$

where F is the flux density of CO_2 (in micromoles per square meter per second), D_s is the gaseous diffusion coefficient of CO_2 in the soil (i.e., soil CO_2 diffusivity in square meters per square second), and $\partial C/\partial z$ is the rate of change of the molar CO_2 concentration (in micromoles per cubic meter) with depth z (i.e., the vertical gradient of soil CO_2 concentration). D_s can be estimated as

$$D_s = D_a \varepsilon \tau \tag{2}$$

where D_a is the CO_2 molecular diffusivity of CO_2 in air, ε is the soil air-filled porosity, and τ is the tortuosity. The product of $\varepsilon\tau$ has been defined as the tortuosity factor ξ (Jury et al. 1991), so that

$$D_s = D_a \xi. \tag{3}$$

The effect of temperature and pressure on D_a is given by

$$D_a = D_{a0} \left(\frac{T}{T_0}\right)^{1.75} \left(\frac{P_0}{P}\right) \tag{4}$$

where D_{a0} is a reference value of D_a (1.47×10^{-5} m^2/s) at T_0 (293.15 K) and P_0 (1.013×10^5 Pa) according to Jones (1992). The tortuosity factor can be calculated using several general models (e.g., Moldrup et al. 1999) or measured and evaluated from an empirical relationship developed for each study site (see Hirano et al. 2003, Pumpanen et al. 2003, Jassal et al. 2005). An accurate determination of the diffusivity factor is essential because CO_2 fluxes are influenced by soil moisture, soil texture, and soil bulk density, all of which affect the diffusivity. In this study, we used the site-specific ξ for sites DF49, HDF88, JP1, JP2, Hyy, and we used the Moldrup model (Moldrup et al. 1999) for the remaining study sites. Although site-specific measurement of the diffusivity is the recommended method, previous studies have found good agreement between F_0 calculated using

TABLE 1. Ancillary information of sites included in this study.

Vegetation type	Site name	Site ID	Latitude, longitude	Country
DF	Hyytiälä	Hyy	61°50′ N, 24°17′ E	Finland
ECF	Blodgett Forest	Blo	38°53′ N, 120°37′ W	USA
	James Reserve		33°48′ N, 116°46′ W	USA
GRA		JRh		
MF		JRw		
	Tonzi Ranch		38°43′ N, 120°96′ W	USA
GRA		TonO		
DF		TonU		
MF	Broadleaf forest	JP1	42°44′ N, 141°44′ E	Japan
ECF	DF49	DF49	49°51′ N, 125°19′ W	Canada
ECF	HDF88	HDF88	49°31′ N, 124°54′ W	Canada
DF	Larch forest	JP2	42°44′ N, 141°31′ E	Japan
GRA	Sevilleta LTER	Sev	34°20′ N, 106°43′ W	USA
GRA	Stubai Valley	Stu	47°07′ N, 11°19′ E	Austria
DF	El Eden	Eden	21°12′ N, 87°11′ W	Mexico

Note: Abbreviations are: DF, deciduous forest dominated by woody vegetation with percent cover >60% and height >2 m and an annual cycle of leaf-on and leaf-off periods; ECF, evergreen coniferous forest land dominated by woody vegetation with percent cover >60% and height >2 m and most trees remain green all year; GRA, grasslands with herbaceous cover, with tree and shrub cover <10%; MF, mixed forests dominated by a mosaic of deciduous and evergreen trees with percent cover >60% and height >2 m; LTER, Long Term Ecological Research center.

TABLE 2. Climate and soil characteristics of sites included in this study.

Site name	Site ID	Elevation (m)	MAP (mm)	MAT (°C)	Soil type	Sand (%)	Silt (%)	Clay (%)	Bulk density (Mg/m^3)	Soil porosity (m^3/m^3)
Hyytiälä	Hyy	181	709	3.8	Haplic podzol	69.2	20	10.8	0.6	0.61
Blodgett Forest	BloC	1315	1290	9	Ultic haploxeralf	60	28	12	0.58	0.78
James Reserve		1640	507	10.3	Entisol	83	10	7		
	JRh								0.9	0.66
	JRw								1.2	0.55
Tonzi Ranch		177	562	16.5	Lithic haploxerepts					
	TonO					48	42	10	1.64	0.38
	TonU					37.5	45	17.5	1.58	0.4
Broadleaf forest	JP1	70	1200	6.5	Volcanogenous regosol	NA	NA	NA	0.42	0.8
DF49†	DF49	300	1320	8.3	Humo-ferric podzol	69.3	22.6	8.1	1.05	0.6
						85.6	13.1	1.3	1.5	0.43
HDF88‡	HDF88	170	1550	9.6	Humo-ferric podzol	39.9	39.9	20.2	0.85	0.68
						41.9	40.2	17.9	0.95	0.64
Larch forest	JP2	140	1250	7.3	Volcanogenous regosol	NA	NA	NA	0.46	0.86
Sevilleta LTER	Sev	1600	250	13.2	Typic Haplargids	68	22	10	1.51	0.43
Stubai Valley	Stu	1850	1097	3	Dystric cambisol	41.9	30.8	27.3	0.91	0.66
El Eden	Eden	10	1650	24.2	Histosol	63	22	15	0.61	0.77

Notes: Soils at JP1 and JP2 are classified as sandy loam, which usually contains 65–85% sand and 0–35% silt, with mean values for sand (75%), silt (18%), and clay (7%). Abbreviations: NA, data not available; MAP, mean annual precipitation, MAT, mean annual temperature; LTER, Long Term Ecological Research center.

† The first set of soil characteristic values is for the 0–10 cm horizon; the second set of values is for the 10–50 cm horizon.

‡ The first set of soil characteristic values is for the 0–10 cm horizon; the second set of values is for the 10–60 cm horizon.

TABLE 1. Extended.

Dominant species	Site history	Main source
Pinus sylvestris	prescribed burning in 1962	Pumpanen et al. (2008)
Pinus ponderosa	plantation established in 1990 after clear-cutting control plot	Tang et al. (2005*b*)
	selective logging until 1966; since then, protected	Vargas and Allen (2008*c*)
Bromus tectorum, *Elymus elymoides*		
Quercus chrysolepis, *Calocedrus decurrens*, *Pinus lambertiana*, *Arctostaphylos pringlei*		
	grazing	Baldocchi et al. (2006)
Brachypodium distachyon, *Bromus hordeaceous*		
Quercus douglasii		
Quercus mongolica, *Magnolia obovata*, *Ulmus davidiana*, *Acer mono*, *Carpinus cordata*	natural forest growing after storm damage by a typhoon in 1954	Hirano et al. (2003)
Pseudotsuga menziesii	slash-burned 1943, planted 1949	Jassal et al. (2005)
Pseudotsuga menziesii	harvested 1987, broadcast burned 1988, planted 1988	Jassal et al. (2008)
Larix kaempferi	the larch forest was planted in 1957–1959	Liang et al. (2004)
Bouteloua eriopoda	human use and cattle grazing until 1973; since then, protected	S. L. Collins, *unpublished data*
Alchemilla vulgaris, *Anthoxanthum odoratum*, *Festuca rubra*, *Leontodon hispidus*, *Trifolium repens*	organic fertilization one cut, grazed in late summer	M. Bahn, *unpublished data*
Bursera simaruba, *Dendropanax arboreus*, *Ficus cotinifolia*, *Guettarda combsii*, *Jatropha gaumeri*, *Lonchocarpus castilloi*, *Lonchocarpus rugosus*, *Nectandra salicifolia*, *Piscidia piscipula*, *Vitex gaumeri*	natural forest growing after fire in 1989 and hurricane disturbance in 2005	Vargas and Allen (2008*a*)

the soil chamber method and F_0 calculated using the flux gradient method of the Moldrup model (Tang et al. 2005*b*, Baldocchi et al. 2006, Vargas and Allen 2008*a*, *b*, *c*).

Assuming a constant rate of CO_2 production in the upper part of the soil profile, F_0 can be calculated as follows (Tang et al. 2005*b*):

$$F_0 = \frac{z_{i+1}F_i - z_iF_{i+1}}{z_{i+1} - z_i} \quad (5)$$

where F_0, F_i, and F_{i+1} are CO_2 effluxes (in micromoles per square meter per second) at depths z_0, z_i, and z_{i+1} (in meters), respectively. This approach has been found to be more reliable than extrapolating the soil CO_2 concentrations to the soil surface and using the gradient between the surface and the first level or taking the derivative of the empirically fit concentration–depth curve at $z = 0$ (Amundson et al. 1998). The condition of constant CO_2 production in the upper part of the soil profile may not be entirely met in productive ecosystems where CO_2 production follows an exponential decay with depth. For each study site we estimated F_i at two depths depending on where the CO_2 sensors were deployed (e.g., between 0.08 and 0.16 m; see Table 3).

Once F_i has been calculated for different levels in the soil profile, P_s can be calculated from the difference between the effluxes across adjacent levels as a flux divergence (Šimůnek and Suarez 1993):

$$P_s = \frac{F_i - F_{i+1}}{z_{i+1} - z_i}. \quad (6)$$

where P_s is the rate of soil CO_2 production (in micromoles per cubic meter per second) in the soil layer between depths i and $i+1$ (Table 3), but the CO_2 storage term was ignored in this equation (see Hirano et al. 2003). We used the shallowest layer in which sensors have been installed to calculate P_s (see Table 3), assuming that these shallow depths have the highest root density (see Jackson et al. 1996). All calculations of F_0 and P_s were performed using mean hourly values and then averaged as daily mean values for further analyses reported in this study. Similarly, hourly values of T_s and θ were averaged as mean daily values and analyses were done using these averages.

Gross primary production

On-site direct measurements of GPP are critical, but we were not able to use GPP derived from eddy covariance towers because not all the sites have these measurements. Thus, to represent the seasonal GPP trend in a systematic way, we used the value-added product derived from MODIS (Running et al. 2004). The product MOD17A2 was used for GPP values (Running et al. 2004), and previous studies have discussed in detail the validation of this product (Turner et al. 2005, Xiao et al. 2005, Zhao et al. 2005, Heinsch et al. 2006). We used MODIS Land Product

TABLE 3. Method used to calculate soil respiration (F_0) and characteristics of soil CO_2 sensor deployments for calculation of soil CO_2 production (P_s) at the study sites.

Site ID, by vegetation type	CO_2 sensor model	Period of measurements	Depth of CO_2 sensors (cm)	Depth of P_s (cm)	F_0 calculation
DF					
Eden	GMM 222	1 Jan to 31 Dec 2005	2, 8, 16	8.5 (2)	flux gradient
JP2	GMD 20	22 Jun 2001 to 22 Jun 2002	0, 2, 11, 13	4.3 (1)	flux gradient
TonU	GMT 222	1 Apr 2003 to 16 Apr 2004	2, 8, 16	8.5 (1)	flux gradient
ECF					
Blo	GMT 222	3 May to 10 Oct 2005	2, 8, 16	8.5 (1)	flux gradient
DF49	GMM 221	13 Mar to 30 Dec 2003	10, 20, 50	25 (3)	automated chambers (6)
HDF88	GMM 221	28 Jul 2005 to 30 Jul 2006	5, 15, 50	21.3 (3)	automated chambers (6)
Hyy	GMP 343	1 Aug 2004 to 17 Jul 2005	0, 5, 17, 27	6.8 (1)	automated chambers (2)
GRA					
JRh	GMM 222	1 Jan to 31 Dec 2006	2, 8, 16	8.5 (4)	flux gradient
Sev	GMM 222	12 Jul to 24 Nov 2007	2, 8, 16	8.5 (3)	flux gradient
Stu	GMT 222	20 Jul 2006 to 20 Jul 2007	5, 10	3.8 (3)	automated chambers (1)
TonO	GMT 222	1 Apr 2003 to 16 Apr 2004	2, 8, 16	8.5 (1)	flux gradient
MF					
JP1	GMD 20	29 May 2000 to 20 May 2001	0, 2, 13, 17	4.3 (1)	flux gradient
JRw	GMM 222	1 Jan 2005 to 31 Dec 2006	2, 8, 16	8.5 (4)	flux gradient

Notes: F_0 was calculated with automated soil respiration chambers or using the flux gradient method. For details on sensor deployment and validation of flux gradients and automated chambers methods see sources in Table 1. Numbers in parentheses represent the number of replicates where P_s was measured. At Stu, F_0 was used to calculate P_s. The flux gradient method has been validated with the chamber method, and calculated F_0 was calibrated spatially with manual and/or automated soil respiration chambers (see sources in Table 1). Abbreviations of vegetation types are: DF, deciduous forest; ECF, evergreen coniferous forest; GRA, grassland; MF, mixed forest. See Table 1 for details on each vegetation type.

Subsets for a 3×3 km grid at each study site using the average of all nine cells. These were derived from MODIS products generated with Collection 4 from the Oak Ridge National Laboratory Distributed Active Archive Center (ORNL DAAC). Details about preparation of subsets including MODIS data reprocessing, methods, and formats are *available online*.[11] Temporal interpolation was used to replace pixels that have quality control flags indicating poor quality. The eight-day MODIS GPP values were extrapolated to daily GPP values (in grams of C per square meter per day) using a Savitzky-Golay smoothing filter. We hereafter refer to the values generated by the product MOD17A2 as GPP.

Analysis of soil CO_2 efflux and production

To test H_1, we calculated mean annual values of the time series of T_s, GPP, F_0, and P_s for each study site and applied linear regression analysis across sites.

To explore the first question and H_2, a cross-correlation analysis using daily mean values between F_0 and T_s or GPP was performed to identify seasonal lags among study sites. Cross-correlation analysis is a measure of similarity of two different measurements as a function of a time lag applied to one of them (Nielsen and Wendroth 2003). In addition, F_0 and P_s were normalized with Eq. 7 to obtain F_0 or P_s at a reference temperature:

$$Y_{15°C} = Y \exp[B_1(15 - T_s)] \quad (7)$$

where Y is either F_0 or P_s, 15°C is the base temperature, and T_s is soil temperature at depth of measured P_s (see Table 3 for depths). Coefficients of nonlinear regressions were estimated using the Levenberg-Marquardt method. A cross-correlation analysis using daily mean values between $F_{015°C}$ or $P_{s15°C}$ and θ was also performed to identify seasonal lag effects among study sites. Finally, we tested how the cross-correlation coefficients between F_0 and T_s or GPP change seasonally with variation in θ.

To explore the second question and H_3 we used an ordination approach using regression tree analysis (Breiman et al. 1984) to represent F_0 or P_s. We used daily mean values of F_0, P_s, T_s, GPP, and θ after including the lags calculated using cross-correlation between variables. Regression tree analysis selects variables that are best able to classify the response (F_0 or P_s) into distinct clusters through a process known as binary recursive partitioning. This is an iterative process of splitting the data into partitions using the predictor variable (T_s, θ, or GPP) that explains the maximum amount of the remaining deviance in the response variable. A minimum node size of 10 was used, meaning no node with fewer than 10 data cases (or data points) was split (Breiman et al. 1984). The advantage of this method is that the tree structure enables interpretation of the explanatory nature of the independent variables. All data analyses were undertaken using MATLAB R2007a (MathWorks, Natick, Massachusetts, USA).

RESULTS

Relationships between F_0 or P_s and T_s or GPP at the annual scale

We did not find significant relationships ($P > 0.1$) between mean annual T_s and mean annual F_0 or mean annual P_s when compared among study sites (Fig. 1A, C).

[11] ⟨http://www.daac.ornl.gov/MODIS/modis.html⟩

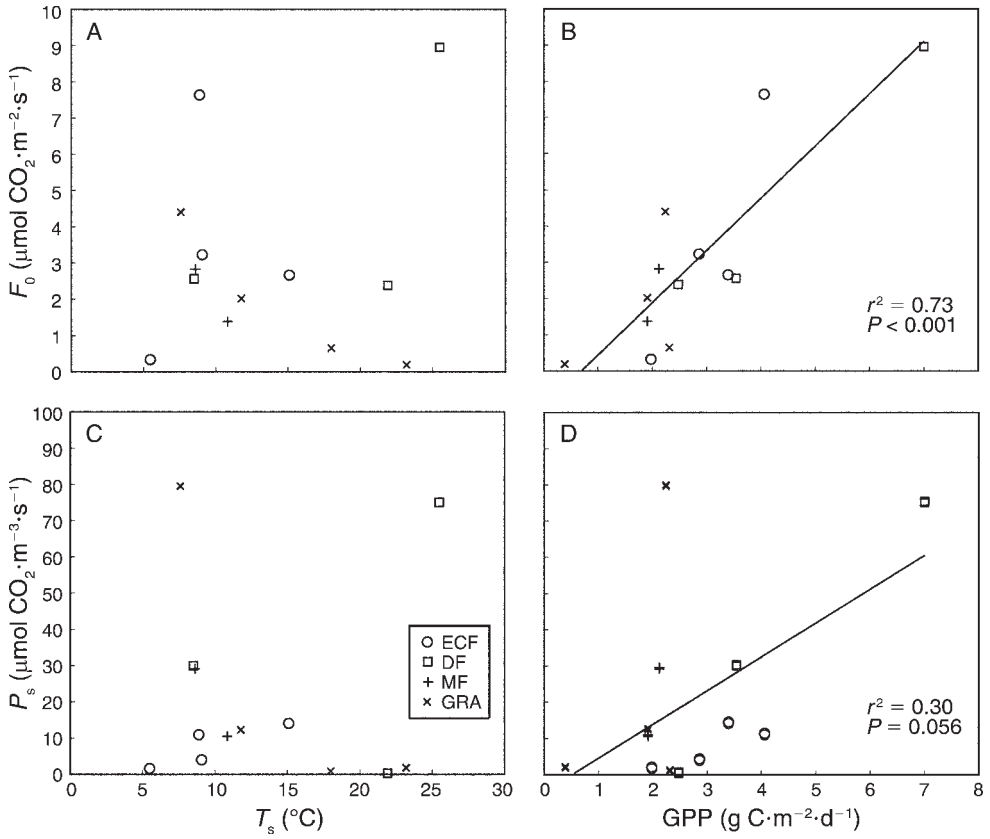

FIG. 1. Across-sites relationships (A, B) between mean annual soil respiration (F_0) and (A) mean annual soil temperature (T_s) and (B) mean annual gross primary production (GPP); and (C, D) between soil CO_2 production (P_s) and (C) mean annual T_s and (D) mean annual GPP among vegetation types. Abbreviations are: ECF, evergreen coniferous forests; DF, deciduous forests; MF, mixed forests; GRA, grasslands. See Table 1 for a summary of the study sites.

In contrast, we observed a significantly positive relationship between mean annual GPP and mean annual F_0 ($P < 0.001$, $r^2 = 0.73$) with a slope of 1.44 ± 0.27 (mean ± SE); this positive relationship was also significant ($P < 0.05$) for deciduous and evergreen coniferous forest sites alone (Fig. 1B). We observed a marginally positive relationship between mean annual GPP and mean annual P_s ($P = 0.056$, $r^2 = 0.30$) with a slope of 9.32 ± 4.4 among all sites, and this positive relationship was also significant ($P < 0.05$) when considering only deciduous and evergreen coniferous forest sites (Fig. 1D).

Cross-correlation analysis

Our results showed that significant ($P < 0.05$) negative lags between 52 and 25 d between F_0 and T_s were associated with deciduous forests, indicating that F_0 increases before T_s at these sites (Table 4). The largest negative lag was at the oak savanna site in California (TonU), with 52 d, followed by a tropical forest in Mexico (Eden), with 36 d. For mixed forests, the largest negative lag was at the California site (JRw), with 24 d. In contrast, for evergreen coniferous forests sites and grassland sites there were no lags, indicating that F_0 was in phase with T_s (Table 4). We observed significant ($P < 0.05$) positive lags between 88 and 5 d between F_0 and GPP in deciduous and mixed forests, indicating that F_0 increases after GPP at these sites (Table 4). For deciduous forests sites, the largest positive lag was at Eden, with 88 d, followed by TonU. For mixed forest the California site (JRw) had a larger positive lag (29 d) than the Japan sites (5 d). For evergreen coniferous forests sites, we observed negative significant ($P < 0.05$) lags between F_0 and GPP, indicating that F_0 increases before GPP at these sites. The largest negative lag was at the Finland site (Hyy), with 24 d, followed by the Canadian site (15 d). In contrast, in grasslands sites, there were no lags, indicating that F_0 was in phase with GPP (Table 4). We analyzed the cross-correlations between $F_{015°C}$ and θ and found no lags ($F_{015°C}$ in phase with θ) at any study site (Table 4). The cross-correlations for P_s with T_s, GPP, or θ showed similar seasonal lags as those found for F_0 at all study sites.

We tested whether the relationship between F_0, T_s, and GPP showed lags based on changes in θ. We found that F_0 and T_s at evergreen coniferous forests and grassland sites were sensitive with negative lags (F_0 peaked before T_s) when θ was >0.3 m^3/m^3 (Fig. 2A). In contrast, the effect of changes in θ on lags between F_0

TABLE 4. Seasonal cross-correlation analyses between daily means of soil respiration (F_0) with daily means of gross primary production (GPP) and daily means of soil temperature (T_s); or daily means of soil respiration at a base temperature reference of 15°C ($F_{15°C}$) with daily means of soil water content (θ).

Site ID by vegetation type	F_0 with GPP	Max. CCC	F_0 with T_s	Max. CCC	$F_{15°C}$ with θ	Max. CCC
DF						
Eden	88	0.40	−36	0.41	0	0.31
JP2	5	0.97	−25	0.87	0	0.48
TonU	21	0.85	−52	0.71	0	0.64
ECF						
Blo	−2	0.65	1	0.58	0	0.56
DF49	−15	0.94	1	0.94	0	0.89
HDF88	−5	0.92	2	0.89	0	0.69
Hyy	−24	0.58	0	0.87	0	0.49
GRA						
JRh	0	0.75	0	0.91	0	0.63
Sev	0	0.19	0	0.35	0	0.56
Stu	0	0.59	0	0.67	0	0.39
TonO	0	0.45	0	0.46	0	0.47
MF						
JP1	5	0.34	0	0.91	0	0.39
JRw	29	0.77	−24	0.81	0	0.69

Notes: A negative lag (in days) means that the maximum cross-correlation coefficient (CCC) ($P < 0.05$) is achieved when F_0 is lagged x number of days before the second variable. A positive lag means that the maximum cross-correlation ($P < 0.05$) coefficient is achieved when F_0 is lagged x number of days after the second variable. A zero lag means that the maximum cross-correlation coefficient is achieved when the time series are not lagged. The maximum cross-correlation coefficients for each site are with $P < 0.05$. See Table 1 for explanations of study site codes.

and GPP was evident when θ was >0.25 m^3/m^3 where evergreen coniferous forests and grasslands showed negative lags, deciduous forests showed positive lags, and mixed forests were not sensitive to changes in θ (Fig. 2B).

Regression trees

The regression trees for F_0 revealed that GPP was the most important parameter for separating high and low values of F_0 in deciduous and evergreen coniferous forest sites with critical values of 3.2 and 7.1 g $C \cdot m^{-2} \cdot d^{-1}$, respectively (Fig. 3A, B). We observed that the second most important variable for deciduous forests was θ, but it was T_s for evergreen coniferous forests. For grasslands, the most important parameter to separate high and low values of F_0 was θ, with a critical value of 0.2 m^3/m^3, while GPP was the secondary variable (Fig. 3C). In contrast, soil temperature was the most important parameter to separate high and low values of F_0 in mixed forests (Fig. 3D). In all cases,

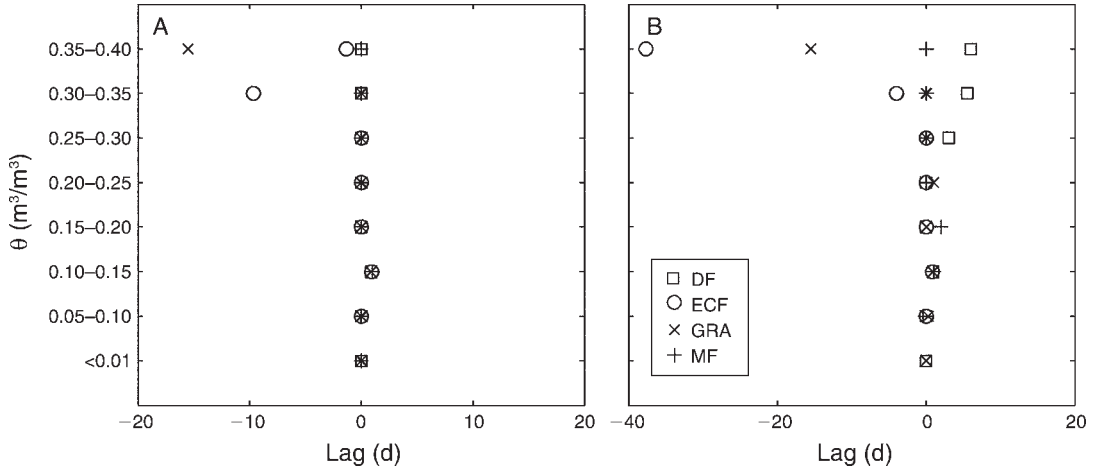

FIG. 2. Effect of soil water content (θ) on lags determined by cross-correlation analysis between (A) daily means of soil respiration (F_0) with daily means of soil temperature (T_s) and (B) daily means of F_0 with gross primary production (GPP). A negative lag means that the maximum cross-correlation coefficient ($P < 0.05$) is achieved when F_0 is lagged x number of days before the second variable. A positive lag means that the maximum cross-correlation ($P < 0.05$) coefficient is achieved when F_0 is lagged x number of days after the second variable. A zero lag means that the maximum cross-correlation coefficient is achieved when the time series are not lagged. Abbreviations are: DF, deciduous forests; ECF, evergreen coniferous forests; GRA, grasslands; and MF, mixed forests.

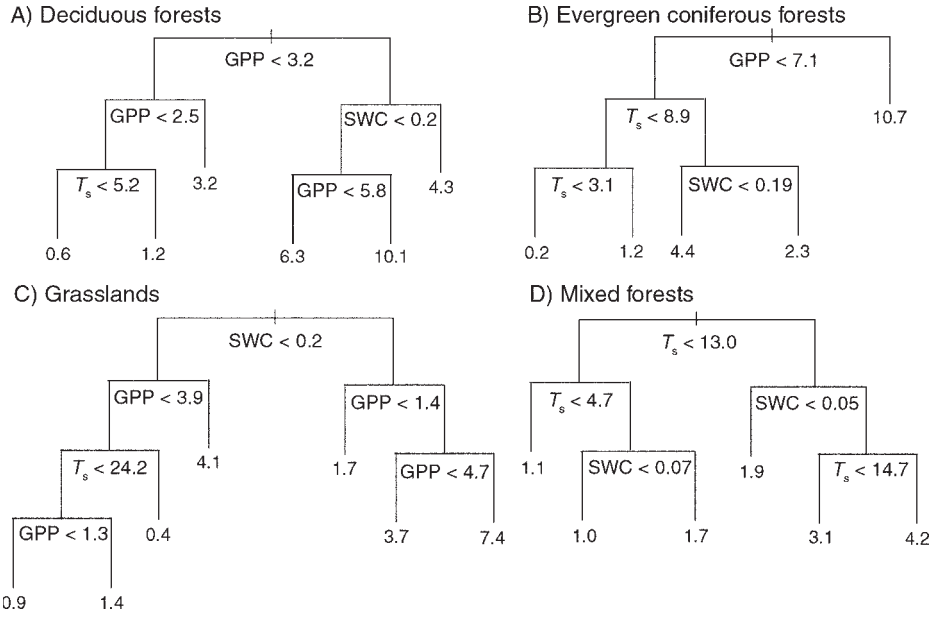

FIG. 3. Regression trees for daily mean soil respiration (F_0) values for: (A) deciduous forests, (B) evergreen coniferous forests, (C) grasslands, and (D) mixed forests. Terminal points of the tree indicate mean F_0 values of the cluster. Abbreviations are: GPP, gross primary production (g $C \cdot m^{-2} \cdot d^{-1}$); T_s, soil temperature (°C); and SWC, soil water content (m^3/m^3).

higher values of all parameters (when important at each node of the tree) discriminated in favor of higher values of F_0. The predicted values of the regression trees for deciduous forests, evergreen coniferous forests, grasslands, and mixed forests explained 67%, 73%, 37%, and 80% of the variance of F_0, respectively. The predicted values of all study sites explained 94% of the variance of all observations of daily F_0 (Fig. 4A).

The regression trees for P_s revealed that GPP was the most important variable for deciduous forests, with a critical value of 4.4 g $C \cdot m^{-2} \cdot d^{-1}$, while θ was a secondary variable associated with higher values of P_s (Fig. 5A). For evergreen coniferous forests, T_s was the most important parameter to separate high and low values of P_s (critical value of 10°C), while GPP was a secondary variable with critical values of 9.7 g $C \cdot m^{-2} \cdot d^{-1}$ for high and 3.4 g $C \cdot m^{-2} \cdot d^{-1}$ for low values of P_s (Fig. 5B). Similarly, T_s was the most important parameter to separate values of P_s in mixed forests with a critical value of 13.1°C, while θ was a secondary variable

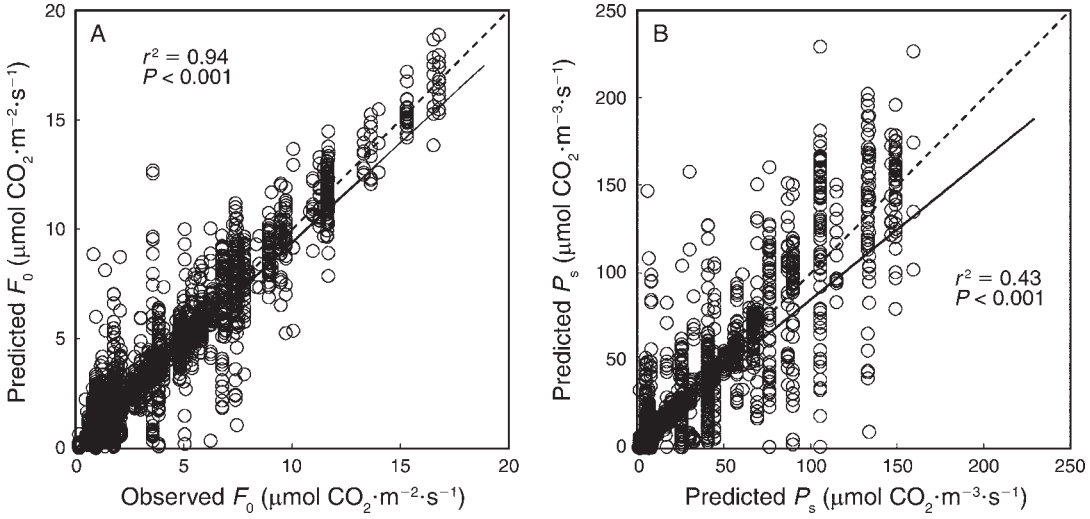

FIG. 4. Daily values of (A) predicted soil respiration (F_0) vs. observed F_0 from regression trees and (B) predicted soil CO_2 production (P_s) vs. observed P_s from regression trees. The dotted line represents an exact 1:1 relationship; the solid line shows the linear regression of these data.

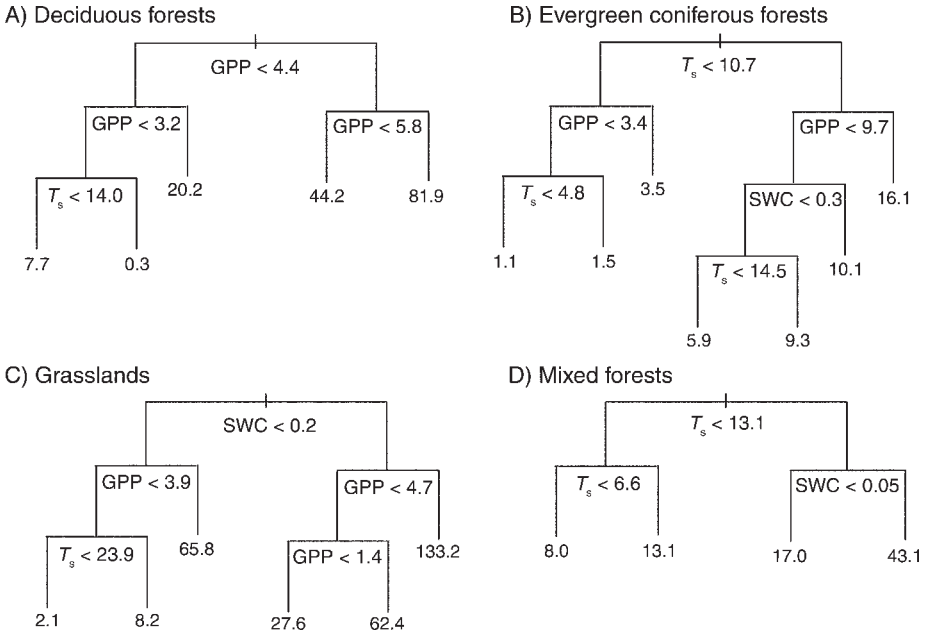

FIG. 5. Regression trees for daily mean soil CO_2 production (P_s) values for: (A) deciduous forests, (B) evergreen coniferous forests, (C) grasslands, and (D) mixed forests. Terminal points of the tree indicate mean P_s values of the cluster. Abbreviations are: GPP, gross primary production (g $C \cdot m^{-2} \cdot d^{-1}$); T_s, soil temperature (°C); and SWC, soil water content (m^3/m^3).

associated with higher values of P_s (Fig. 5D). In contrast, θ was the most important variable in grasslands (critical value of 0.2 m^3/m^3), while GPP was a secondary variable (Fig. 5C). In all cases higher values of all parameters (when important at each node of the tree) discriminated in favor of higher values of P_s. The predicted values of the regression trees for deciduous forests, evergreen coniferous forests, grasslands, and mixed forests explained 47%, 33%, 32%, and 77% of the variance of P_s, respectively. Consequently, the overall predicted values of all study sites explained 43% of the variance of all observations of daily P_s and underestimate higher values of P_s (Fig. 4B).

DISCUSSION

Are there seasonal lags between F_0 and T_s, θ, or GPP, and if so, do these lags differ among vegetation types?

Biological systems respond to present and past input stimulus, thus processes regulating soil CO_2 fluxes can be studied as causal or non-anticipatory systems. Identifying lags is important to the understanding of the manner in which biophysical factors influence processes that regulate variation in terrestrial CO_2 fluxes (e.g., Braswell et al. 1997). Here, we focus on seasonal lags (cross-correlation analysis between two one-year-long time series), and our results support the hypothesis that lags between F_0 with T_s and GPP provide insights into the role of plant phenology and potentially about the timing of processes associated with autotrophic and heterotrophic components of soil respiration at the seasonal scale.

Seasonal lags between F_0 and T_s cause seasonal hysteresis effects that are evident in deciduous, evergreen coniferous, and mixed forest. The amplitude of the seasonal hysteresis and the lag between the time series may depend on the different timing and contributions of autotrophic and heterotrophic components of F_0 (Drewitt et al. 2002, Vargas and Allen 2008*c*). For example, seasonal soil CO_2 fluxes at deciduous and mixed forest sites responded after an increase in photosynthesis (positive lags with GPP) but before a peak in temperature (negative lags with T_s). Thus it is likely that at these sites the seasonal pattern of F_0 is driven first by a substantial increase in autotrophic activity (after inputs from GPP), followed by an increase in heterotrophic activity (after inputs from GPP and an increase in T_s). These results support previous observations in which photosynthesis (Baldocchi et al. 2006), phenology (DeForest et al. 2006), and root–rhizomorph dynamics (Burton et al. 1998, Vargas and Allen 2008*c*) played a role in regulating seasonal soil CO_2 fluxes at deciduous and mixed forest sites.

For evergreen coniferous forests (located at high altitudes or latitudes), F_0 increases in phase with T_s but before GPP (Table 4). At these sites, the seasonal pattern of F_0 may be driven first by a substantial increase in heterotrophic activity (after an increase in T_s) followed by an increase in autotrophic activity (after an increase in T_s and inputs from GPP). Our results support previous observations in which photosynthesis (Högberg et al. 2001) and temperature (Pumpanen et al. 2008) were found to regulate soil CO_2 fluxes in boreal forests.

For grasslands we observed that F_0 was in phase with seasonal variation in T_s and GPP because soil CO_2 fluxes respond rapidly to changes in photosynthesis and

assimilate supply in short-stature vegetation (Bahn et al. 2008, 2009). This apparent ectothermic pattern in grasslands suggests that the seasonal pattern of F_0 may be regulated by a coupled seasonal timing of autotrophic and heterotrophic activity. The seasonal lags presented in this study must be compared using a larger network of sites across multiple climatic zones and vegetation types, and it is critical to partition the contribution to F_0 by autotrophic and heterotrophic activity using stable isotopes and radiocarbon (Carbone et al. 2008, Bahn et al. 2009) at multiple temporal scales. Only with direct measurements can we clearly demonstrate the magnitude of the contribution of each component of soil CO_2 fluxes.

We have discussed seasonal lags between soil CO_2 fluxes and T_s or GPP during the year, but the temporal correlation between these variables could change at shorter timescales, depending on the season and changes in θ. We found that higher θ values (>0.3 m^3/m^3) influence the intra-seasonal time lags between F_0 and T_s or GPP. These high values could be associated with periods of snowmelt and precipitation events that change the diffusivity of CO_2 in the soil, increase nutrient solution in the soil, and influence the photosynthesis rates at the ecosystem scale (Huxman et al. 2004, Xu and Baldocchi 2004). High water levels can also constrain root and microbial metabolism by reducing oxygen availability for respiration. To understand water pulse dynamics it is important to understand how changes in θ influence soil CO_2 fluxes and their associated biophysical factors (Irvine and Law 2002, Jassal et al. 2008). Further research is needed to identify lags at multiple temporal scales and to understand the biophysical mechanisms that control them in multiple vegetation types.

We believe it is important to include lags in empirical and biogeochemical models to better represent the variation of soil CO_2 fluxes. A simple example could be the modification of the empirical relationship between T_s and F_0 by including lags at the appropriate temporal scale:

$$F_0 = B_0 \times \exp(B_1 \times T_s^{(\lambda)}) \quad (8)$$

where $T_s^{(\lambda)}$ is the time series of T_s lagged by the appropriate time step (e.g., lag in days for a seasonal scale or lag in hours for a daily timescale). The inclusion of lags in seasonal estimations of F_0 based on T_s could reduce potential errors associated with diel and seasonal hysteresis effects (Vargas and Allen 2008*c*).

What are the relationships and interactions among F_0, T_s, θ, and GPP within different vegetation types?

Our results showed that mean annual GPP was a good predictor for mean annual F_0 and P_s among our study sites. This result supports previous observations in which GPP overshadows T_s in determining soil and ecosystem respiration in European forest (Janssens et al. 2001), grasslands (Bahn et al. 2008), and among FLUXNET sites (Reichstein et al. 2003, Baldocchi et al. 2006). The fact that there was a strong relationship between F_0 and GPP derived independently from remote sensing provides motivation for further studies using GPP derived from remote-sensing platforms.

It is important to recognize that MODIS GPP values represent a different footprint than the site-specific measurements of CO_2 fluxes; therefore future studies must require a dense spatial array of soil CO_2 measurements to corroborate the results presented in this study. In most cases F_0 was calibrated spatially using manual soil respiration chambers (see references in Table 1), but may not fully represent the MODIS subset in which GPP was estimated. This is a current challenge as there is a trade-off between frequency of measurements (e.g., daily) and spatial coverage (e.g., plot level vs. landscape) that is limited by human resources, electrical power, and budget. Despite these limitations our results encourage the application of MODIS products for the estimation of soil CO_2 fluxes at large geographical distances. Further studies should compile larger data sets and test these observations among sites with different soil, vegetation, and climatic conditions that could help in future global estimates of soil CO_2 fluxes.

Cross-correlation analysis showed distinct time lags for each vegetation type, providing insights about the timing of soil CO_2 processes. We applied respective lags in the time series, and regression tree analyses showed that the dominant environmental factors influencing soil CO_2 fluxes differ between vegetation types. Using daily values, we found that GPP was the dominant variable explaining the variance in F_0 for deciduous and evergreen coniferous forests, but was the second most important variable for grasslands. In contrast, T_s was the main variable for mixed forests while θ was the dominant variable for grasslands as these are mainly from arid or semiarid regions (but see Bahn et al. 2008). It is known that in arid and Mediterranean ecosystems, precipitation pulses dictate microbial dynamics influencing CO_2 fluxes (Ogle and Reynolds 2004, Xu et al. 2004, Kurc and Small 2007, Collins et al. 2008). However, for the mesic grassland site (Stu) GPP was the main regulator of soil CO_2 fluxes (data not shown), supporting the importance of this variable in temperate mesic grasslands (Bahn et al. 2008). From regression trees, we could generalize that increased GPP is linked with higher soil CO_2 fluxes, and when T_s and θ are relevant, they also promote higher values of F_0 and P_s among all vegetation types.

Although we found similar patterns and relationships that regulate F_0 and P_s, a low percentage of the variance (43%) in P_s was explained by regression trees in comparison with the 90% explained for F_0. We present two complementary explanations: (1) parameters other than T_s, GPP, and θ are needed to explain the variance in P_s, and (2) there is a larger mismatch between GPP and P_s because it is difficult to spatially average biophysical processes that act deeper in the soil.

Because P_s is a measurement of biological activity, we postulate that other unmeasured factors, likely of biological origin, may not be fully explained by GPP, T_s, and θ alone (Kuzyakov 2006). Previous studies have shown that fine roots and mycorrhizal rhizomorph dynamics (Misson et al. 2006, Heinemeyer et al. 2007, Gaumont-Guay et al. 2008, Vargas and Allen 2008*c*) and substrate supply and nutrient availability (Schimel et al. 1994, Ruess et al. 2003) are other biological drivers that influence P_s. To date we do not have a common biological variable (other than GPP) among sites (e.g., root production, microbial biomass) that could allow us to test this hypothesis. It is a current challenge to spatially average the biophysical processes that interact deeper in the soil profile, but this information is critical for improving climate models as these processes could influence the regional climate (Lee et al. 2005).

Limitations and future considerations

To better understand the drivers of soil CO_2 fluxes, it is necessary to study the distribution of P_s in the soil profile. Although we assumed a constant P_s with soil depth and analyzed P_s values calculated for a shallow depth with higher root density zones, future studies should determine the depth of maximum CO_2 production. This is why it is critical to look deeper into the soil to understand the biophysical drivers of P_s suggested in this study. Multiple CO_2 sensors in the soil profile allow the calculation of P_s at multiple depths to understand the different contributions over the soil profile (Hashimoto and Suzuki 2002, Hirano et al. 2003, Jassal et al. 2005, Davidson et al. 2006). High spatial sampling resolution is important to understand vertical and horizontal variation in F_0 and P_s (Vargas and Allen 2008*a*, *c*), especially in complex terrains (Riveros-Iregui et al. 2008). Furthermore, measurement points should follow indicators of biological activity (e.g., maximum root biomass or maximum rooting depth) or biophysical transitions in the soil (e.g., soil horizons) associated with T_s and θ measurements to better interpret P_s at individual sites or across sites (Pumpanen et al. 2008). We recognize that the flux-gradient method is not always the most appropriate method to estimate F_0 in all conditions, and more studies are needed to compare methods and calculate P_s at multiple depths. However, values of F_0 obtained using different methods (autochambers vs. flux gradient method) have been shown to yield similar results within the sites included in this study (Tang et al. 2003, 2005*b*, Liang et al. 2004, Jassal et al. 2005, Baldocchi et al. 2006, Pumpanen et al. 2008, Vargas and Allen 2008*a*, *b*, *c*).

Finally, studies that incorporate complementary measurements are needed to understand the controls of P_s on F_0. Examples are the combination of soil CO_2 concentration measurements with soil respiration autochambers (Jassal et al. 2005, 2008, Pihlatie et al. 2007), eddy covariance towers (Baldocchi et al. 2006), minirhizotron measurements (Misson et al. 2006, Vargas and Allen 2008*b*, *c*), or the possibility of incorporating analyses of natural abundance of radiocarbon (Carbone et al. 2008) and stable isotopes (Bahn et al. 2009) in soil CO_2 fluxes. With increasing interest in wireless networks (Allen et al. 2007, Porter et al. 2009) and the emergence of long-term automated soil sensor networks as a result of continental monitoring programs (e.g., FLUXNET, NEON, ICOS), complex spectral analysis of continuous biometeorological measurements can be applied (Vargas et al., *in press*). We expect that these regional networks and future analyses will provide critical data and input parameters for testing process-based models among multiple vegetation types.

Acknowledgments

We greatly appreciate the many collaborators and colleagues who have helped collect the data. In particular we thank Renee Brown, Juan Castillo, Kuni Kitajima, Niles Hasselquist, Liisa Kulmala, Siyan Ma, and Michael Schmitt. John Battles and Diego Riveros-Iregui provided helpful comments that improved this work. Data collection was possible thanks to NASA, the NSF Center for Embedded Networked Sensing (CCR-0120778), DOE (DE-FG02-03ER63638), CONACyT, UCMEXUS, NSF (EF-0410408), NSF-LTER, KAKENHI (12878089 and 13480150), the Academy of Finland (213093), the Austrian Science Fund (FWF, P18756-B16), the Kearney Foundation, the Canadian Foundation for Climate and Atmospheric Sciences (CFCAS), and the Natural Science and Engineering Research Council of Canada (NSERC). R. Vargas was supported by grant DEB-0639235 during the preparation of this manuscript. Financial support does not constitute an endorsement by the funding agencies of the views expressed in this article. The initial collaboration for this work was established thanks to a workshop organized by the research coordination network Terrestrial Ecosystem Response to Atmospheric and Climatic Change (TERACC).

Literature Cited

Allen, M. F., R. Vargas, E. A. Graham, W. Swenson, M. P. Hamilton, M. Taggart, T. C. Harmon, A. Rat'ko, P. W. Rundel, B. Fulkerson, and D. L. Estrin. 2007. Soil sensor technology: life within a pixel. BioScience 57:859–867.

Amundson, R., L. Stern, T. Baisden, and Y. Wang. 1998. The isotopic composition of soil and soil-respired CO_2. Geoderma 82:83–114.

Bahn, M., M. Knapp, Z. Garajova, N. Pfahringer, and A. Cernusca. 2006. Root respiration in temperate mountain grasslands differing in land use. Global Change Biology 12: 995–1006.

Bahn, M., M. Schmitt, R. Siegwolf, A. Richter, and N. Bruggemann. 2009. Does photosynthesis affect grassland soil-respired CO_2 and its carbon isotope composition on a diurnal timescale? New Phytologist 182:451–460.

Bahn, M., et al. 2008. Soil respiration in European grasslands in relation to climate and assimilate supply. Ecosystems 11: 1352–1367.

Baldocchi, D. 2008. Breathing of the terrestrial biosphere: lessons learned from a global network of carbon dioxide flux measurement systems. Australian Journal of Botany 56:1–26.

Baldocchi, D., J. W. Tang, and L. K. Xu. 2006. How switches and lags in biophysical regulators affect spatial-temporal variation of soil respiration in an oak–grass savanna. Journal of Geophysical Research 111:G02008.

Braswell, B. H., D. S. Schimel, E. Linder, and B. Moore. 1997. The response of global terrestrial ecosystems to interannual temperature variability. Science 278:870–872.

Breiman, L., J. H. Friedman, R. A. Olshen, and C. J. Stone. 1984. Classification and regression trees. Wadsworth and Brooks/Cole, Monterey, California, USA.

Burton, A. J., K. S. Pregitzer, G. P. Zogg, and D. R. Zak. 1998. Drought reduces root respiration in sugar maple forests. Ecological Applications 8:771–778.

Carbone, M. S., G. C. Winston, and S. E. Trumbore. 2008. Soil respiration in perennial grass and shrub ecosystems: linking environmental controls with plant and microbial sources on seasonal and diel timescales. Journal of Geophysical Research 113:G02022.

Collins, S. L., R. L. Sinsabaugh, C. Crenshaw, L. Green, A. Porras-Alfaro, M. Stursova, and L. H. Zeglin. 2008. Pulse dynamics and microbial processes in aridland ecosystems. Journal of Ecology 96:413–420.

Curiel Yuste, J., I. A. Janssens, A. Carrara, L. Meiresonne, and R. Ceulemans. 2003. Interactive effects of temperature and precipitation on soil respiration in a temperate maritime pine forest. Tree Physiology 23:1263–1270.

Davidson, E. A., and I. A. Janssens. 2006. Temperature sensitivity of soil carbon decomposition and feedbacks to climate change. Nature 440:165–173.

Davidson, E. A., K. E. Savage, S. E. Trumbore, and W. Borken. 2006. Vertical partitioning of CO_2 production within a temperate forest soil. Global Change Biology 12:944–956.

Davidson, E. A., and S. E. Trumbore. 1995. Gas diffusivity and production of CO_2 in deep soils of the eastern Amazon. Tellus, Series B, Chemical and Physical Meteorology 47:550–565.

Davidson, E. A., L. V. Verchot, J. H. Cattanio, I. L. Ackerman, and J. E. M. Carvalho. 2000. Effects of soil water content on soil respiration in forests and cattle pastures of eastern Amazonia. Biogeochemistry 48:53–69.

DeForest, J. L., A. Noormets, S. G. McNulty, G. Sun, G. Tenney, and J. Q. Chen. 2006. Phenophases alter the soil respiration–temperature relationship in an oak-dominated forest. International Journal of Biometeorology 51:135–144.

DeJong, E., and H. J. V. Schapper. 1972. Calculation of soil respiration and activity from CO_2 profiles in the soil. Soil Science 113:328–333.

Drewitt, G. B., T. A. Black, Z. Nesic, E. R. Humphreys, E. M. Jork, R. Swanson, G. J. Ethier, T. Griffis, and K. Morgenstern. 2002. Measuring forest floor CO_2 fluxes in a Douglas-fir forest. Agricultural and Forest Meteorology 110: 299–317.

Fierer, N., O. A. Chadwick, and S. E. Trumbore. 2005. Production of CO_2 in soil profiles of a California annual grassland. Ecosystems 8:412–429.

Gaumont-Guay, D., T. A. Black, A. G. Barr, R. S. Jassal, and Z. Nesic. 2008. Biophysical controls on rhizospheric and heterotrophic components of soil respiration in a boreal black spruce stand. Tree Physiology 28:161–171.

Gaumont-Guay, D., T. A. Black, T. J. Griffis, A. G. Barr, R. S. Jassal, and Z. Nesic. 2006. Interpreting the dependence of soil respiration on soil temperature and water content in a boreal aspen stand. Agricultural and Forest Meteorology 140:220–235.

Goulden, M. L., and P. M. Crill. 1997. Automated measurements of CO_2 exchange at the moss surface of a black spruce forest. Tree Physiology 17:537–542.

Hanson, P. J., N. T. Edwards, C. T. Garten, and J. A. Andrews. 2000. Separating root and soil microbial contributions to soil respiration: a review of methods and observations. Biogeochemistry 48:115–146.

Hashimoto, S., and H. Komatsu. 2006. Relationships between soil CO_2 concentration and CO_2 production, temperature, water content, and gas diffusivity: implications for field studies through sensitivity analyses. Journal of Forest Research 11:41–50.

Hashimoto, S., and M. Suzuki. 2002. Vertical distributions of carbon dioxide diffusion coefficients and production rates in forest soils. Soil Science Society of America Journal 66:1151–1158.

Heinemeyer, A., I. P. Hartley, S. P. Evans, J. A. C. De la Fuente, and P. Ineson. 2007. Forest soil CO_2 flux: uncovering the contribution and environmental responses of ectomycorrhizas. Global Change Biology 13:1786–1797.

Heinsch, F. A., et al. 2006. Evaluation of remote sensing based terrestrial productivity from MODIS using regional tower eddy flux network observations. IEEE Transactions on Geoscience and Remote Sensing 44:1908–1925.

Hibbard, K. A., B. E. Law, M. Reichstein, and J. Sulzman. 2005. An analysis of soil respiration across northern hemisphere temperate ecosystems. Biogeochemistry 73:29–70.

Hirano, T., H. Kim, and Y. Tanaka. 2003. Long-term half-hourly measurement of soil CO_2 concentration and soil respiration in a temperate deciduous forest. Journal of Geophysical Research 108:4631.

Högberg, P., A. Nordgren, N. Buchmann, A. F. S. Taylor, A. Ekblad, M. N. Hogberg, G. Nyberg, M. Ottosson-Lofvenius, and D. J. Read. 2001. Large-scale forest girdling shows that current photosynthesis drives soil respiration. Nature 411: 789–792.

Huxman, T. E., K. A. Snyder, D. Tissue, A. J. Leffler, K. Ogle, W. T. Pockman, D. R. Sandquist, D. L. Potts, and S. Schwinning. 2004. Precipitation pulses and carbon fluxes in semiarid and arid ecosystems. Oecologia 141:254–268.

Irvine, J., and B. E. Law. 2002. Contrasting soil respiration in young and old-growth ponderosa pine forests. Global Change Biology 8:1183–1194.

Jackson, R. B., J. Canadell, J. R. Ehleringer, H. A. Mooney, O. E. Sala, and E. D. Schulze. 1996. A global analysis of root distributions for terrestrial biomes. Oecologia 108:389–411.

Janssens, I. A., et al. 2001. Productivity overshadows temperature in determining soil and ecosystem respiration across European forests. Global Change Biology 7:269–278.

Jassal, R. S., T. A. Black, G. B. Drewitt, M. D. Novak, D. Gaumont-Guay, and Z. Nesic. 2004. A model of the production and transport of CO_2 in soil: predicting soil CO_2 concentrations and CO_2 efflux from a forest floor. Agricultural and Forest Meteorology 124:219–236.

Jassal, R. S., T. A. Black, M. D. Novak, D. Gaumont-Guay, and Z. Nesic. 2008. Effect of soil water stress on soil respiration and its temperature sensitivity in an 18-year-old temperate Douglas-fir stand. Global Change Biology 14: 1305–1318.

Jassal, R., T. A. Black, M. Novak, K. Morgenstern, Z. Nesic, and D. Gaumont-Guay. 2005. Relationship between soil CO_2 concentrations and forest-floor CO_2 effluxes. Agricultural and Forest Meteorology 130:176–192.

Jones, H. G. 1992. Plants and microclimate: a quantitative approach to environmental plant physiology. Cambridge University Press, New York, New York, USA.

Jury, W. A., W. R. Gardner, and W. H. Gardner. 1991. Soil physics. Wiley, New York, New York, USA.

Kurc, S. A., and E. E. Small. 2007. Soil moisture variations and ecosystem-scale fluxes of water and carbon in semiarid grassland and shrubland. Water Resources Research 43: W06416.

Kuzyakov, Y. 2006. Sources of CO_2 efflux from soil and review of partitioning methods. Soil Biology and Biochemistry 38: 425–448.

Lee, J. E., R. S. Oliveira, T. E. Dawson, and I. Fung. 2005. Root functioning modifies seasonal climate. Proceedings of the National Academy of Sciences USA 102:17576–17581.

Liang, N. S., T. Nakadai, T. Hirano, L. Y. Qu, T. Koike, Y. Fujinuma, and G. Inoue. 2004. In situ comparison of four approaches to estimating soil CO_2 efflux in a northern larch (*Larix kaempferi* Sarg.) forest. Agricultural and Forest Meteorology 123:97–117.

Liu, Q., N. T. Edwards, W. M. Post, L. Gu, J. Ledford, and S. Lenhart. 2006. Temperature-independent diel variation in soil respiration observed from a temperate deciduous forest. Global Change Biology 12:2136–2145.

Ma, S. Y., J. Q. Chen, J. R. Butnor, M. North, E. S. Euskirchen, and B. Oakley. 2005. Biophysical controls on soil respiration in the dominant patch types of an old-growth, mixed-conifer forest. Forest Science 51:221–232.

Magnani, F., et al. 2007. The human footprint in the carbon cycle of temperate and boreal forests. Nature 447:848–850.

McDowell, N. G., D. R. Bowling, B. J. Bond, J. Irvine, B. E. Law, P. Anthoni, and J. R. Ehleringer. 2004. Response of the carbon isotopic content of ecosystem, leaf, and soil respiration to meteorological and physiological driving factors in a *Pinus ponderosa* ecosystem. Global Biogeochemical Cycles 18:GB1013.

Misson, L., A. Gershenson, J. W. Tang, M. McKay, W. X. Cheng, and A. Goldstein. 2006. Influences of canopy photosynthesis and summer rain pulses on root dynamics and soil respiration in a young ponderosa pine forest. Tree Physiology 26:833–844.

Moldrup, P., T. Olesen, T. Yamaguchi, P. Schjonning, and D. E. Rolston. 1999. Modeling diffusion and reaction in soils. IX. The Buckingham-Burdine-Campbell equation for gas diffusivity in undisturbed soil. Soil Science 164:542–551.

Nielsen, D. R., and O. Wendroth. 2003. Spatial and temporal statistics: sampling field soils and their vegetation. Catena-Verlag, Reiskirchen, Germany.

Ogle, K., and J. F. Reynolds. 2004. Plant responses to precipitation in desert ecosystems: integrating functional types, pulses, thresholds, and delays. Oecologia 141:282–294.

Pihlatie, M., J. Pumpanen, J. Rinne, H. Ilvesniemi, A. Simojoki, P. Hari, and T. Vesala. 2007. Gas concentration driven fluxes of nitrous oxide and carbon dioxide in boreal forest soil. Tellus, Series B, Chemical and Physical Meteorology 59:458–469.

Porter, J. H., E. Nagy, T. K. Kratz, P. Hanson, S. L. Collins, and P. Arzberger. 2009. New eyes on the world: advanced sensors for ecology. BioScience 59:385–397.

Pumpanen, J., H. Ilvesniemi, and P. Hari. 2003. A process-based model for predicting soil carbon dioxide efflux and concentration. Soil Science Society of America Journal 67: 402–413.

Pumpanen, J., H. Ilvesniemi, L. Kulmala, E. Siivola, H. Laakso, P. Kolari, C. Helenelund, M. Laakso, M. Uusimaa, and P. Hari. 2008. Respiration in boreal forest soil as determined from carbon dioxide concentration profile. Soil Science Society of America Journal 72:1187–1196.

Pumpanen, J., et al. 2004. Comparison of different chamber techniques for measuring soil CO_2 efflux. Agricultural and Forest Meteorology 123:159–176.

Raich, J. W., C. S. Potter, and D. Bhagawati. 2002. Interannual variability in global soil respiration, 1980–94. Global Change Biology 8:800–812.

Reichstein, M., et al. 2003. Modeling temporal and large-scale spatial variability of soil respiration from soil water availability, temperature and vegetation productivity indices. Global Biogeochemical Cycles 17:1104.

Risk, D., L. Kellman, and H. Beltrami. 2002. Carbon dioxide in soil profiles: production and temperature dependence. Geophysical Research Letters 29:1087.

Riveros-Iregui, D. A., B. L. McGlynn, H. E. Epstein, and D. L. Welsch. 2008. Interpretation and evaluation of combined measurement techniques for soil CO_2 efflux: discrete surface chambers and continuous soil CO_2 concentration probes. Journal of Geophysical Research 113:G04027.

Ruess, R. W., R. L. Hendrick, A. J. Burton, K. S. Pregitzer, B. Sveinbjornsson, M. E. Allen, and G. E. Maurer. 2003. Coupling fine root dynamics with ecosystem carbon cycling in black spruce forests of interior Alaska. Ecological Monographs 73:643–662.

Running, S. W., R. R. Nemani, F. A. Heinsch, M. S. Zhao, M. Reeves, and H. Hashimoto. 2004. A continuous satellite-derived measure of global terrestrial primary production. BioScience 54:547–560.

Ryan, M. G., and B. E. Law. 2005. Interpreting, measuring, and modeling soil respiration. Biogeochemistry 73:3–27.

Savage, K. E., and E. A. Davidson. 2003. A comparison of manual and automated systems for soil CO_2 flux measurements: trade-offs between spatial and temporal resolution. Journal of Experimental Botany 54:891–899.

Schimel, D. S., B. H. Braswell, E. A. Holland, R. McKeown, D. S. Ojima, T. H. Painter, W. J. Parton, and A. R. Townsend. 1994. Climatic, edaphic, and biotic controls over storage and turnover of carbon in soils. Global Biogeochemical Cycles 8:279–293.

Šimůnek, J., and D. L. Suarez. 1993. Modeling of carbon-dioxide transport and production in soil. 1. Model development. Water Resources Research 29:487–497.

Takahashi, A., T. Hiyama, H. A. Takahashi, and Y. Fukushima. 2004. Analytical estimation of the vertical distribution of CO_2 production within soil: application to a Japanese temperate forest. Agricultural and Forest Meteorology 126:223–235.

Tang, J. W., D. D. Baldocchi, Y. Qi, and L. K. Xu. 2003. Assessing soil CO_2 efflux using continuous measurements of CO_2 profiles in soils with small solid-state sensors. Agricultural and Forest Meteorology 118:207–220.

Tang, J., D. D. Baldocchi, and L. Xu. 2005*a*. Tree photosynthesis modulates soil respiration on a diurnal time scale. Global Change Biology 11:1298–1304.

Tang, J., L. Misson, A. Gershenson, W. X. Cheng, and A. H. Goldstein. 2005*b*. Continuous measurements of soil respiration with and without roots in a ponderosa pine plantation in the Sierra Nevada Mountains. Agricultural and Forest Meteorology 132:212–227.

Turner, D. P., et al. 2005. Site-level evaluation of satellite-based global terrestrial gross primary production and net primary production monitoring. Global Change Biology 11:666–684.

Vargas, R., and M. F. Allen. 2008*a*. Diel patterns of soil respiration in a tropical forest after Hurricane Wilma. Journal of Geophysical Research, Biogeosciences 113: G03021.

Vargas, R., and M. F. Allen. 2008*b*. Dynamics of fine root, fungal rhizomorphs, and soil respiration in a mixed temperate forest: integrating sensors and observations. Vadose Zone Journal 7:1055–1064.

Vargas, R., and M. F. Allen. 2008*c*. Environmental controls and the influence of vegetation type, fine roots and rhizomorphs on diel and seasonal variation in soil respiration. New Phytologist 179:460–471.

Vargas, R., M. Detto, D. D. Baldocchi, and M. F. Allen. 2010 Multiscale analysis of temporal variability of soil CO_2 production as influenced by weather and vegetation. Global Change Biology. 16:1589–1605.

Xiao, X. M., Q. Y. Zhang, D. Hollinger, J. Aber, and B. Moore. 2005. Modeling gross primary production of an evergreen needleleaf forest using MODIS and climate data. Ecological Applications 15:954–969.

Xu, L. K., and D. D. Baldocchi. 2004. Seasonal variation in carbon dioxide exchange over a Mediterranean annual grassland in California. Agricultural and Forest Meteorology 123:79–96.

Xu, L. K., D. D. Baldocchi, and J. W. Tang. 2004. How soil moisture, rain pulses, and growth alter the response of ecosystem respiration to temperature. Global Biogeochemical Cycles 18:GB4002.

Zhao, M. S., F. A. Heinsch, R. R. Nemani, and S. W. Running. 2005. Improvements of the MODIS terrestrial gross and net primary production global data set. Remote Sensing of Environment 95:164–176.